Weissel, J., Peirce, J., Taylor, E., Alt, J., et al., 1991
Proceedings of the Ocean Drilling Program, Sci. Results, Vol. 121

43. *DATA REPORT:* IRIDIUM AND TRACE ELEMENT MEASUREMENTS FROM THE CRETACEOUS-TERTIARY BOUNDARY, SITE 752, BROKEN RIDGE, INDIAN OCEAN[1]

B. C. Schuraytz,[2] S. O'Connell,[3] and V. L. Sharpton[2]

ABSTRACT

Fourteen samples spanning a 2.5 m interval that includes the Cretaceous-Tertiary (K/T) boundary from Hole 752B near the crest of Broken Ridge in the eastern Indian Ocean, were studied in order to search for anomalous enrichments of iridium (Ir) and shock-metamorphosed quartz grains. No allogenic quartz grains >10 μm were observed, hence the presence of quartz containing diagnostic evidence of shock-metamorphism could not be confirmed. Two Ir anomalies of 2.2±0.6 and 2.0±0.4 parts per billion (ppb) were measured in samples of dark green ash-bearing chalk at depths of 357.93 and 358.80 m below seafloor (mbsf), respectively, (Samples 121-752B-11R-3, 13–14 cm, and 121-752B-11R-3, 100–101 cm) using conventional Instrumental Neutron Activation Analysis (INAA). These samples containing anomalous enrichments of Ir were taken from approximately 82 cm above and 5 cm below the extinction level of Globotruncanids. Our results are consistent with those of Michel et al. (this volume), who observe elevated concentrations of Ir at these depths in addition to a larger Ir anomaly associated with the extinction level of Globotruncanids.

INTRODUCTION

Following the discovery of excess iridium (Ir) at the Cretaceous/Tertiary (K/T) boundary in European sections and its interpretation as geochemical evidence that a major impact event caused the massive and abrupt extinction event marking the end of the Mesozoic Era (Alvarez et al., 1980; Ganapathy, 1980), considerable attention has been devoted to understanding the nature of the K/T boundary. In accordance with the "impact hypothesis," it soon was recognized that the K/T boundary layer also contained other siderophile elements in proportions that were distinctly unlike the differentiated components of Earth's crust but were strikingly similar to undifferentiated extraterrestrial material such as C1 chondrite (Ganapathy, 1980; Alvarez et al., 1982). This geochemical signature appears to be global in extent (Alvarez et al., 1982; 1984), and, at least in some well-preserved sites, is singular, discrete, and distinctly unlike any other stratigraphic layer deposited in the last 70 m.y. (Kyte and Wasson, 1986; Kyte, 1988). Independent evidence of impact, in the form of shock-deformed mineral grains, also has been detected at many sites world-wide (Bohor et al., 1984; 1987). Natural occurrences of such deformation have been demonstrated through laboratory and field studies to be unique to meteorite impact (see Sharpton and Schuraytz, 1989, and references therein).

While such unequivocal evidence of a major impact event at the K/T boundary suggests the mass extinctions were induced by the impact, several observations have been advanced in challenge to this hypothesis. These include reports of multiple Ir anomalies (Crockett et al., 1988; Rocchia et al., 1988; Graup et al., 1989) and paleontological evidence of extended or precursory extinctions at some sites (Keller, 1989). Several investigators (Officer and Drake, 1985; Hallam, 1987; Officer et al., 1987) have argued that these and other characteristics of the K/T boundary are in closer accordance with a more extended period of intense volcanic eruptions than with an instantaneous event such as meteorite impact (cf. Alvarez et al., 1984). Assessment of available age determinations led Courtillot et al. (1990) to propose that the Deccan Traps erupted in several distinct phases beginning in the late Maestrichtian and that such intense episodes of basaltic activity could generate these global biological and geochemical effects. Other explanations for multiple anomalies, however, include a barrage of comets spanning 1–3 m.y. (Hut et al., 1987), post-depositional processes (Graup et al., 1989), and/or sample bias effects (Signor and Lipps, 1982). More detailed documentation of existing K/T sections and identification and assessment of new sites is required before the relative significance of impact (single or multiple), volcanic activity, and preservation effects can be adequately resolved.

Our ongoing study focuses on detailed characterizations of 34 samples at and around the K/T boundary at five ODP sites in the Indian Ocean. In this short note we present geochemical data for the 14 samples spanning a 2.5 m interval containing the K/T boundary from Hole 752B near the crest of Broken Ridge in the eastern Indian Ocean.

REGIONAL SETTING

Site 752 is located in the eastern Indian Ocean, near the crest of Broken Ridge in 1,086 m of water (Fig. 1). A continuous K/T boundary was recovered within a 60-cm-long ash-chert-chalk sequence (Fig. 2) in Core 121-752B-11R, 358.2–358.8 mbsf (Pierce, Weissel, et al., 1989). Recovery in Core 11R was 56% and consisted of 4- to 10-cm-long cylinders or "drilling biscuits."

Below the boundary interval, the Maestrichtian sediments consist primarily of mottled chalk of varying shades of gray. The actual boundary interval, based on the extinction of Globotruncanids is most likely to be between 73 and 95 cm in Section 121-752B-11R-3, 358.5–358.7 mbsf (Pierce, Weissel, et al., 1989). The boundary interval is contained within and is immediately overlain by a compound ash layer which is greater than 5.5 m thick.

SAMPLING AND ANALYTICAL PROCEDURES

A total of 14 samples, approximately 2–3 cm^3 in size, were selected in order to obtain a representative sampling of visible lithological variations and distinct breaks within the 2.5 m interval of core that contains the K/T boundary as identified by the

[1] Weissel, J., Peirce, J., Taylor, E., Alt, J., et al., 1991.. *Proc. ODP, Sci. Results,* 121: College Station, TX (Ocean Drilling Program).
[2] Lunar and Planetary Institute, 3303 NASA Rd. 1, Houston, TX 77058, U.S.A.
[3] Department of Earth and Environmental Sciences, Wesleyan University, Middletown, CT 06457, U.S.A.

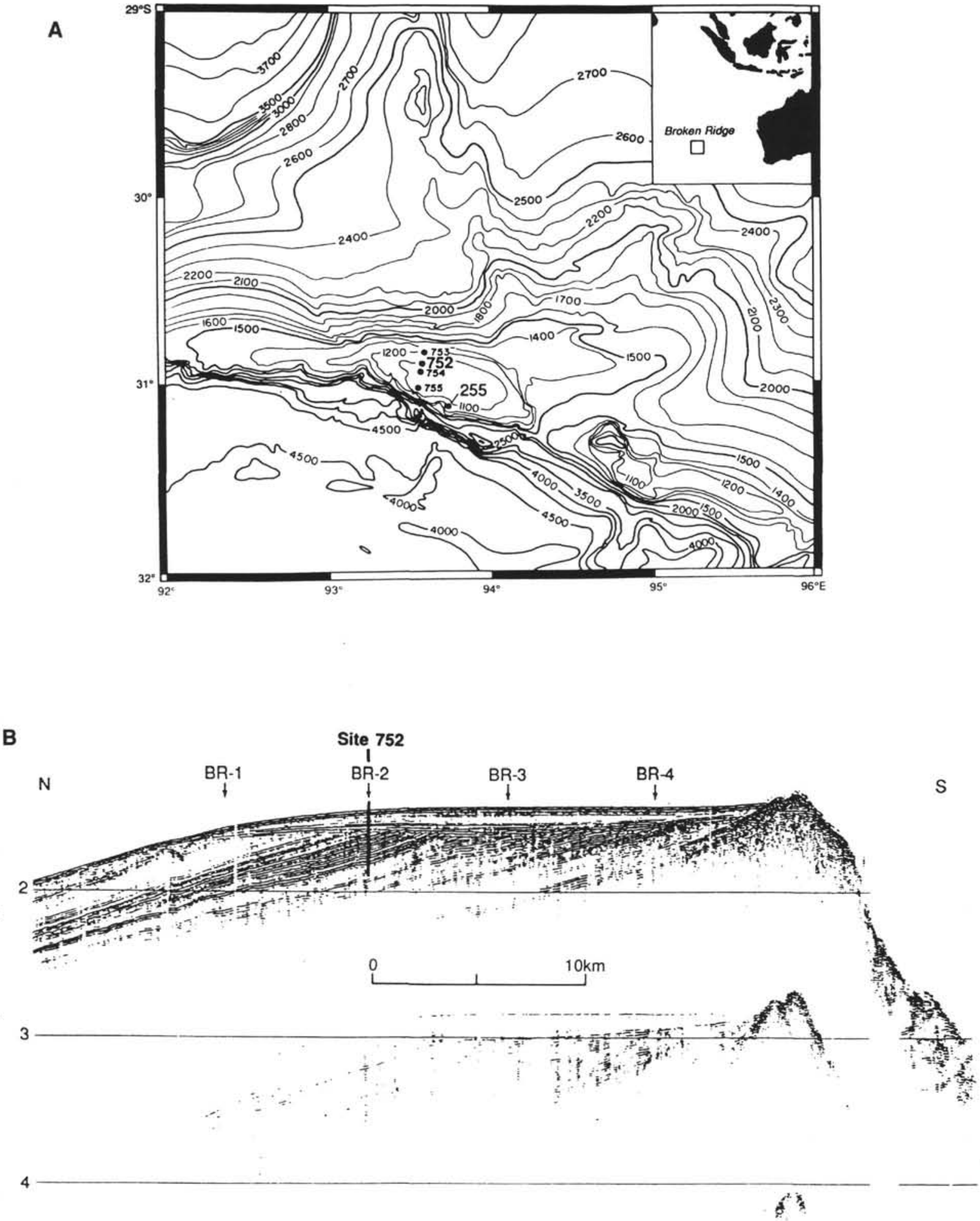

Figure 1. **A.** Bathymetric map showing location of Site 752. Contours at 100-m intervals, except along the south-facing escarpment where contours are omitted for clarity. **B.** Single channel seismic-reflection profile (RC2708 line 20) across Broken Ridge showing the location of Site 752 (Pierce, Weissel, et al., 1989).

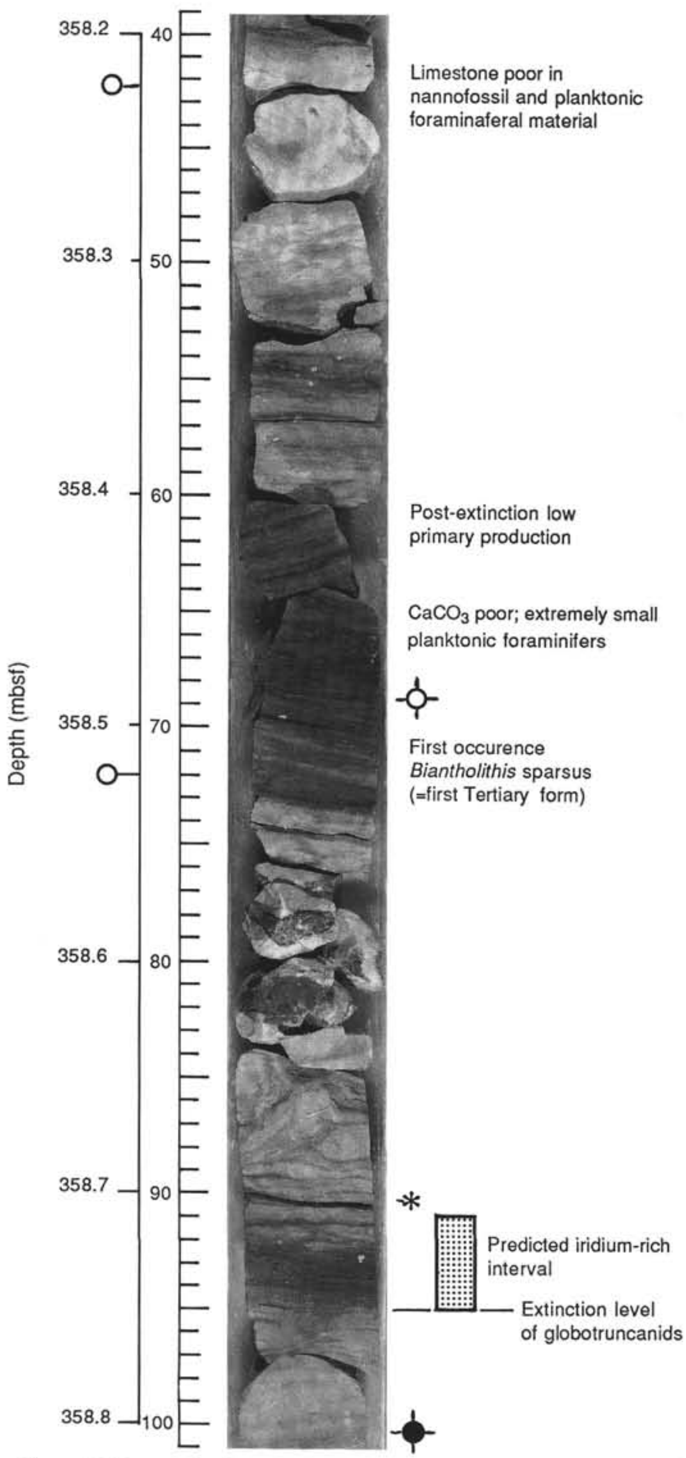

Figure 2. Photograph of core containing the K/T boundary. The boundary interval lies between 72 and 95 cm in Section 121-752B-11R-3. Locations of samples analyzed in this study are shown by circles; open circle = Ir below detection; solid circle = anomalous enrichment of Ir; cross projecting from circle = dark and light sediment analyzed separately. The location of Sample 121-752B-11R-2, 76–77 cm, is not shown. Additional information about sample locations is given in Table 1 and Ir values are presented in Table 2. Star denotes location of maximum Ir peak meassured by Michel et al. (this volume).

Shipboard Party (Fig. 2, Table 1). Sample size and spacing were constrained by the amount of material available and by JOIDES (Joint Oceanographic Institutions for Deep Earth Sampling) sampling guidelines. Samples were numbered randomly and split. One split was gently crushed and examined in immersion oil using a petrographic microscope. The other split was powdered by hand with an agate mortar and pestle for chemical analysis by conventional INAA. Where a distinct color difference existed within a sample and where the different colored material could be separated, the sample was further subdivided to preserve the color integrity, and two separate samples (denoted A and B, respectively) were analyzed. In addition, one sample (121-752B-11R-3, 13–14 cm) was analyzed twice (T19-1 and T19-2) to provide a check on the reproducibility of results.

Homogenized rock powder from each sample was sealed in a silica tube and irradiated at the University of Missouri Research reactor with a flux of 4.90×10^{13} n cm^{-2} s^{-1} for 14 hr. Counting and data reduction was done at the NASA Johnson Space Center using recently upgraded equipment and data reduction techniques (Lindstrom and Korotev, 1982; D. Lindstrom and D. Mittlefehldt, unpubl. program, 1988). U.S. Geological Survey (USGS) AN-G was used as the standard for sodium and calcium; USGS DTS-1 for iron, chromium, cobalt, and nickel; South African Bureau of Standards SARM-7 for iridium and gold; and U.S. National Bureau of Standards NBS-1633A for all other elements.

RESULTS

Abundances of 30 elements within each of the analyzed samples are presented in Table 2. The analytical uncertainties presented ($\pm 1\sigma$) take into account the propagation of errors due to counting statistics, uncertainties of elemental abundances in the standards, and sample/detector geometry. Limits of detection are governed by counting time and the composition of the sample, and thus will vary among samples. In cases where an element was below the limit of detection (i.e., the number of counts in the region of interest was not sufficiently above the background to distinguish a statistically significant peak), a value indicating the 2σ upper limit for the abundance of that element is shown enclosed in parentheses (Table 2).

Ir was detected in 2 of the 14 samples analyzed, at abundances of 2.2±0.6 and 2.0±0.4 ppb. Upper limits (2σ) for the 12 samples in which no Ir was detected range from <0.3 to <1.1 ppb. Michel et al. (this volume) determined an average background level of 0.022 ppb Ir below the K/T boundary using an Iridium Coincidence Spectrometer (ICS), which is more sensitive than the single detector used in our conventional INAA procedure. Hence, Ir abundances at the 2 ppb level are substantially above background and indicate anomalous enrichments of Ir in these samples.

An Ir abundance of 2.0±0.4 ppb was measured in dark green sediment from 121-752B-11R-3, 100–101 cm (Table 2, sample T21B). This sample occurs 5 cm below the extinction level of Globotruncanids and approximately 8 cm below the maximum Ir peak of 3.8 ppb identified by Michel et al. (this volume). Ir values of their closest samples, obtained at approximately 1 cm above and 4 cm below our sample, (0.098 and 0.862 ppb, respectively) indicate our sample represents a distinct "spike" in Ir abundance rather than the tail of the main K/T anomaly.

A second Ir anomaly was detected in a sample from 121-752B-11R-3, 13–14 cm. This sample was analyzed in two splits (Table 2, samples T19-1 and T19-2), with Ir abundances of 2.7±1.0 ppb and 1.9±0.8 ppb, respectively. These values agree within analytical uncertainty, and yield a weighted mean abundance of 2.2±0.6 ppb. This sample, which also consists of dark green sediment, occurs approximately 82 cm above the extinction level of Globotruncanids. Michel et al. (this volume) detected an Ir anomaly of 1.5 ppb at the same location in the core.

Table 1. Descriptions of core samples from Hole 752B. The darker samples contain more clay minerals and the lighter samples contain more chalk.

ID number	Core, section, interval (cm)	Depth (mbsf)	Color and comments
TT28	11R-2, 76–77	357.06	dark green
T19	11R-3, 13–14	357.93	dark green (two splits analyzed)
TT29	11R-3, 24–25	358.04	fine layering
TT27	11R-3, 27–28	358.07	green
TT32	11R-3, 34–35	358.14	layered green
T24	11R-3, 42–43	358.22	very hard sediment
TT31	11R-3, 67–68	358.47	dark and light sediment, mostly light sampled
T26A	11R-3, 73–74	358.53	dark green
T26B	11R-3, 73–74	358.53	light green
T21A	11R-3, 100–101	358.80	light green
T21B	11R-3, 100–101	358.80	dark green
T23	11R-3, 120–121	359.00	very hard sediment
T22	11R-3, 140–141	359.20	abundant dark speckles
T20	11R-4, 13–14	359.43	light green

No allogenic quartz grains >10 mm were observed in the petrographic analysis of the samples. Therefore, the presence of quartz containing diagnostic evidence of shock-metamorphism (Sharpton and Grieve, 1990) could not be confirmed. However, our investigations were severely hindered by the limited amount of material available for this search.

SUMMARY

We were successful in detecting anomalous enrichments of Ir in the vicinity of the K/T boundary at Site 752; therefore, the data in Table 2 provide useful information regarding geochemical distinctions between the Ir-enriched horizons and the adjacent regional sediments. We note that the Ir distribution obtained in our analysis is consistent with that of Michel et al. (this volume) based on a different sampling strategy and a different analytical technique. Because we could not obtain a sample of material at the extinction level of Globotruncanids as defined by the Shipboard Party, we cannot comment on the distribution of Ir and shock-deformed minerals precisely at the K/T boundary. However, the occurrence of two additional Ir anomalies in close proximity to the K/T boundary suggests that either a single Ir-rich horizon has been redistributed or that the Ir was deposited in more than one episode.

ACKNOWLEDGMENTS

We thank the staff of the Gulf Coast Repository for their assistance in sampling these cores. The INAA work was done through cooperation of the INAA Laboratory at NASA Johnson Space Center and we thank D. Mittlefehldt for his assistance. The Lunar and Planetary Institute is operated by the Universities Space Research Association under Contract No. NASW-4066 with the National Aeronautics and Space Administration. Partial funding for this study was provided by USSAC. This is Lunar and Planetary Institute Contribution No. 755.

REFERENCES

Alvarez, L. W., Alvarez, W., Asaro, F., and Michel, H. V., 1980. Extraterrestrial cause for the Cretaceous-Tertiary extinction. *Science,* 208:1095–1107.

Alvarez, W., Alvarez, L. W., Asaro, F., and Michel, H. V., 1982. Current status of the impact theory for the terminal Cretaceous extinction. *In* Silver, L. T., and Schultz, P. H. (Eds.), *Geological Implications of Impacts of Large Asteroids and Comets on the Earth.* Spec. Pap. Geol. Soc. Am., 190:305–315.

———, 1984. The end of the Cretaceous: sharp boundary or gradual transition. *Science,* 233:1183–1186.

Bohor, B. F., Foord, E. E., Modreski, P. J., and Triplehorn, D. M., 1984. Mineralogical evidence for an impact event at the Cretaceous-Tertiary boundary. *Science,* 244:867–869.

Bohor, B. F., Modreski, P. J., and Foord, E. E., 1987. Shocked quartz in the Cretaceous-Tertiary boundary clay: evidence for a global distribution. *Science,* 236:705–709.

Courtillot, V., Besse, J., Vandamme, D., Jaeger, J. J., Javoy, M., Feraud, G., Maluski, H., and Rocchia, R., in press. Deccan volcanism at the Cretaceous-Tertiary boundary: data and inferences. *In* Sharpton, V. L., and Ward, P. D. (Eds.), *Global Catastrophes in Earth History: An Interdisciplinary Conference on Impacts, Volcanoes and Mass Mortality.* Spec. Pap. Geol. Soc. Am., 247.

Crocket, J. H., Officer, C. B., Wezel, F. C., and Johnson, G. D., 1988. Distribution of noble metals across the Cretaceous/Tertiary boundary at Gubbio, Italy: iridium variations as a constraint on the duration and nature of Cretaceous/Tertiary boundary events. *Geology,* 16:77–80.

Ganapathy, R., 1980. A major meteorite impact on the earth 65 million years ago: evidence from the Cretaceous-Tertiary boundary clay. *Science,* 209:921–923.

Graup, G., Spettel, G., Herm, D., and Weidich, D. F., 1989. Mineralogy and phase-chemistry of an Ir-enriched pre-K/T layer from the Lattengebirge, Bavarian Alps, and significance for the KTB problem. *Earth Planet. Sci. Lett.,* 95:271–290.

Hallam, A., 1987. The end-Cretaceous mass extinction event: argument for terrestrial cause. *Science,* 238:1237–1242.

Hut, P., Alvarez, W., Hansen, T. Kaufmann, D., Keller, G., Shoemaker, E., and Weissman, P., 1987. Comet showers as a cause of mass extinctions, *Nature,* 329: 118–126.

Keller, G., 1989. Extended period of extinctions across the Cretaceous/Tertiary boundary in planktonic foraminifera of continental-shelf sections: implications for impact and volcanism theories. *Geol. Soc. Am. Bull.,* 101:1408–1419.

Kyte, F. T., 1988. Accretion rate of extraterrestrial matter: iridium deposited over the last 70 million years. *Global Catastrophes in Earth History: An Interdisciplinary Conference on Impacts, Volcanoes, and Mass Mortality.* Houston (Lunar and Planetary Inst.), 101. (Abstract)

Kyte, F. T., and Wasson, J. T., 1986. Accretion rate of extraterrestrial matter: iridium deposited 33 to 67 million years ago. *Science,* 232:1225–1229.

Lindstrom, D. J., and Korotev, R. L., 1982. TEABAGS: computer programs for instrumental neutron activation analysis. *J. Radioanal. Chem.,* 70:439–458.

Officer, C. B., and Drake, C. L., 1985. Terminal Cretaceous environmental events. *Science,* 227:1161–1167.

Officer, C. B., Hallam, A., Drake, C. L., and Devine, J. D., 1987. Late Cretaceous and paroxysmal Cretaceous/Tertiary extinctions. *Nature,* 326:143–149.

Peirce, J., Weissel, J., et al., 1989. *Proc. ODP, Init. Repts.,* 121: College Station, TX (Ocean Drilling Program).

Rocchia, R., Boclet, D., Buffetaut, E., Orne-Extebarria, X., Jaeger, J. J., and Jehanno, C., 1988. Structure of the iridium anomaly at the K-T boundary of the Sopelana section (Spanish Basque country). *C. R. Acad. Sci. Paris,* 30:1217.

Sharpton, V. L., and Grieve, R.A.F., in press. Meteorite impact, cryptoexplosion, and shock metamorphism: a perspective on the evidence at the K/T boundary. *In* Sharpton, V. L., and Ward, P. D. (Eds.), *Global Catastrophes in Earth History: An Interdisciplinary Conference on Impacts, Volcanoes and Mass Mortality.* Spec. Pap. Geol. Soc. Am., 247.

Sharpton, V. L., and Schuraytz, B. C., 1989. On reported occurrences of shock-deformed clasts in the volcanic ejecta from Toba caldera, Sumatra. *Geology,* 17:1040–1043.

Shipboard Scientific Party, 1989. Cretaceous/Tertiary boundary summary. *In* Peirce, J., Weissel, J., et al., *Proc. ODP, Init. Repts.,* 121: College Station, TX (Ocean Drilling Program), 507–516.

Signor, P. W., III, and Lipps, J. H., 1982. Sampling bias, gradual extinction patterns, and catastrophes in the fossil record. *In* Silver, L. T., and Schultz, P. H. (Eds.), *Geological Implications of Impacts of Large Asteroids and Comets on the Earth.* Spec. Pap. Geol. Soc. Am., 190:291–296.

Date of initial receipt: 20 May 1990
Date of acceptance: 27 November 1990
Ms 121B-175

Table 2. Chemical analyses of core samples from Hole 752B obtained by INAA. Analytical uncertainties are ± 1μ. Upper limits (2μ) for abundances below detection are enclosed in parentheses.

Sample ID	TT28	T19-1	T19-2	TT29	TT27	TT32	T24	TT31
Depth (mbsf)	357.06	357.93	357.93	358.04	358.07	358.14	358.22	358.47
Mass (mg)	118.8	58.70	131.6	109.0	100.3	110.3	119.3	83.25
Weight percent								
Na_2O	2.72 ± 0.04	1.807 ± 0.021	1.910 ± 0.026	1.761 ± 0.023	1.498 ± 0.020	1.845 ± 0.024	0.410 ± 0.005	2.061 ± 0.026
K_2O	1.45 ± 0.25	2.41 ± 0.25	2.41 ± 0.24	1.60 ± 0.15	1.52 ± 0.24	1.75 ± 0.18	0.218 ± 0.017	0.85 ± 0.08
CaO	5.8 ± 0.9	16.6 ± 0.4	16.5 ± 0.9	19.3 ± 0.6	22.4 ± 0.5	19.0 ± 0.6	39.0 ± 0.7	19.5 ± 0.7
FeO	10.19 ± 0.11	7.65 ± 0.08	7.62 ± 0.08	4.72 ± 0.05	3.80 ± 0.04	5.26 ± 0.06	0.488 ± 0.006	7.37 ± 0.08
Parts per million								
Sc	25.36 ± 0.28	22.57 ± 0.25	22.80 ± 0.25	15.86 ± 0.17	14.82 ± 0.16	16.58 ± 0.18	1.644 ± 0.018	19.95 ± 0.22
Cr	32.9 ± 0.6	63.5 ± 0.9	63.9 ± 0.9	53.8 ± 0.8	33.4 ± 0.5	31.4 ± 0.5	2.76 ± 0.13	65.0 ± 0.9
Co	31.0 ± 0.4	26.0 ± 0.3	27.5 ± 0.3	13.22 ± 0.16	10.37 ± 0.12	12.17 ± 0.15	3.44 ± 0.04	24.06 ± 0.28
Ni	43 ± 13	76 ± 14	67 ± 11	40 ± 9	27 ± 8	48 ± 13	(<12)	46 ± 12
Rb	21.2 ± 1.7	39.2 ± 1.9	38.7 ± 1.7	20.8 ± 1.2	23.4 ± 1.2	27.2 ± 1.4	3.1 ± 0.3	11.8 ± 1.4
Cs	0.31 ± 0.03	0.77 ± 0.04	0.75 ± 0.03	0.363 ± 0.028	0.404 ± 0.027	0.40 ± 0.03	0.057 ± 0.010	0.19 ± 0.03
Sr	1040 ± 40	820 ± 30	830 ± 30	1250 ± 40	1220 ± 40	1140 ± 40	411 ± 24	730 ± 30
Ba	1454 ± 28	443 ± 13	478 ± 12	4410 ± 80	4440 ± 80	3840 ± 70	885 ± 17	1960 ± 40
La	9.29 ± 0.12	25.68 ± 0.29	26.08 ± 0.29	15.78 ± 0.18	21.46 ± 0.24	22.26 ± 0.25	13.67 ± 0.15	12.25 ± 0.14
Ce	18.30 ± 0.28	40.8 ± 0.6	40.4 ± 0.5	27.4 ± 0.4	35.4 ± 0.5	41.6 ± 0.6	20.7 ± 0.3	16.24 ± 0.26
Nd	10.3 ± 2.0	22.3 ± 2.4	25.7 ± 2.1	14.1 ± 1.5	19.8 ± 1.8	25.1 ± 2.1	11.5 ± 1.0	9.2 ± 1.7
Sm	3.32 ± 0.05	5.38 ± 0.07	5.49 ± 0.07	3.57 ± 0.05	4.69 ± 0.07	5.86 ± 0.08	1.914 ± 0.024	2.75 ± 0.04
Eu	1.016 ± 0.018	1.288 ± 0.023	1.350 ± 0.22	0.779 ± 0.015	0.993 ± 0.016	1.133 ± 0.020	0.275 ± 0.006	0.778 ± 0.016
Tb	0.663 ± 0.022	1.032 ± 0.028	1.058 ± 0.025	0.614 ± 0.019	0.777 ± 0.019	1.048 ± 0.025	0.288 ± 0.008	0.580 ± 0.021
Yb	2.39 ± 0.04	3.43 ± 0.05	3.45 ± 0.05	1.87 ± 0.03	2.61 ± 0.04	3.47 ± 0.05	1.148 ± 0.020	1.98 ± 0.03
Lu	0.362 ± 0.008	0.494 ± 0.011	0.502 ± 0.009	0.281 ± 0.006	0.384 ± 0.008	0.510 ± 0.009	0.160 ± 0.003	0.302 ± 0.006
Zr	133 ± 22	103 ± 22	121 ± 20	87 ± 16	115 ± 17	203 ± 27	67 ± 8	68 ± 19
Hf	2.77 ± 0.06	2.68 ± 0.07	2.66 ± 0.05	2.19 ± 0.05	2.95 ± 0.06	4.82 ± 0.09	1.82 ± 0.04	1.88 ± 0.05
Ta	0.432 ± 0.016	0.554 ± 0.020	0.577 ± 0.017	0.507 ± 0.015	0.740 ± 0.018	1.330 ± 0.030	0.666 ± 0.017	0.332 ± 0.016
U	0.31 ± 0.06	0.38 ± 0.05	0.32 ± 0.05	0.64 ± 0.05	0.52 ± 0.07	1.60 ± 0.07	0.086 ± 0.017	0.87 ± 0.05
Th	1.05 ± 0.03	1.37 ± 0.04	1.418 ± 0.029	1.61 ± 0.03	2.61 ± 0.04	4.47 ± 0.07	2.28 ± 0.03	0.900 ± 0.029
As	(<1.0)	1.45 ± 0.18	1.70 ± 0.25	0.29 ± 0.12	(<0.6)	0.54 ± 0.18	0.19 ± 0.03	1.58 ± 0.12
Se	0.50 ± 0.21	(<0.6)	(<0.4)	(<0.7)	0.34 ± 0.17	(<0.8)	(<0.31)	1.41 ± 0.24
Sb	0.376 ± 0.020	0.748 ± 0.022	0.762 ± 0.020	0.236 ± 0.013	0.555 ± 0.018	0.769 ± 0.020	0.164 ± 0.005	0.427 ± 0.017
Parts per billion								
Ir	(<1.0)	2.7 ± 1.0	1.9 ± 0.8	(<0.8)	(<0.8)	(<0.9)	(<0.8)	(<1.1)
Au	1.7 ± 0.8	3.3 ± 1.2	3.7 ± 1.4	3.4 ± 1.0	3.7 ± 1.4	3.5 ± 1.2	1.0 ± 0.4	2.7 ± 1.0

Table 2 (continued).

Sample ID	T26A	T26B	T21A	T21B	T23	T22	T20
Depth (mbsf)	358.53	358.53	358.80	358.80	359.00	359.20	359.43
Mass (mg)	105.1	125.0	145.5	105.6	126.4	149.9	121.2
Weight percent							
Na_2O	1.319 ± 0.017	1.178 ± 0.015	0.550 ± 0.006	0.789 ± 0.011	0.451 ± 0.006	0.425 ± 0.005	0.458 ± 0.006
K_2O	0.85 ± 0.15	0.80 ± 0.07	0.68 ± 0.07	0.52 ± 0.11	0.31 ± 0.04	0.28 ± 0.03	0.41 ± 0.04
CaO	28.3 ± 0.6	32.0 ± 0.9	43.2 ± 0.8	39.2 ± 0.7	42.5 ± 0.7	41.7 ± 0.7	43.3 ± 0.8
FeO	3.01 ± 0.03	2.96 ± 0.03	1.092 ± 0.012	1.430 ± 0.016	0.542 ± 0.006	0.438 ± 0.005	0.689 ± 0.008
Parts per million							
Sc	16.08 ± 0.18	15.22 ± 0.17	4.29 ± 0.05	6.27 ± 0.07	2.84 ± 0.03	2.276 ± 0.025	3.03 ± 0.03
Cr	56.8 ± 0.8	53.9 ± 0.7	9.30 ± 0.23	38.0 ± 0.6	5.96 ± 0.17	5.15 ± 0.13	7.25 ± 0.20
Co	32.8 ± 0.4	20.85 ± 0.25	6.71 ± 0.08	22.42 ± 0.26	2.96 ± 0.04	2.247 ± 0.028	5.28 ± 0.06
Ni	43 ± 10	26 ± 7	23 ± 4	64 ± 6	10 ± 3	(<12)	10 ± 4
Rb	11.7 ± 1.0	12.7 ± 0.9	10.4 ± 0.6	9.7 ± 0.7	6.0 ± 0.4	5.4 ± 0.4	7.2 ± 0.4
Cs	0.260 ± 0.029	0.249 ± 0.026	0.306 ± 0.014	0.349 ± 0.020	0.243 ± 0.012	0.212 ± 0.010	0.257 ± 0.013
Sr	920 ± 30	746 ± 28	1060 ± 40	990 ± 40	960 ± 50	940 ± 50	980 ± 60
Ba	3450 ± 60	2420 ± 40	1173 ± 22	743 ± 15	1066 ± 21	1128 ± 22	1398 ± 27
La	19.23 ± 0.22	17.99 ± 0.20	14.29 ± 0.16	13.81 ± 0.16	11.69 ± 0.13	11.10 ± 0.12	11.54 ± 0.13
Ce	20.8 ± 0.3	18.90 ± 0.27	10.68 ± 0.16	12.30 ± 0.19	7.86 ± 0.13	7.12 ± 0.12	8.29 ± 0.14
Nd	16.1 ± 1.9	12.8 ± 1.2	11.7 ± 1.0	12.7 ± 1.3	11.1 ± 1.0	10.1 ± 0.9	11.5 ± 1.0
Sm	3.62 ± 0.05	3.25 ± 0.04	2.38 ± 0.03	2.78 ± 0.04	1.958 ± 0.025	1.807 ± 0.023	1.938 ± 0.025
Eu	0.936 ± 0.016	0.835 ± 0.015	0.572 ± 0.010	0.643 ± 0.011	0.451 ± 0.008	0.408 ± 0.007	0.445 ± 0.008
Tb	0.620 ± 0.021	0.614 ± 0.016	0.394 ± 0.010	0.499 ± 0.013	0.346 ± 0.010	0.320 ± 0.009	0.328 ± 0.009
Yb	2.36 ± 0.04	2.15 ± 0.03	1.380 ± 0.021	2.03 ± 0.03	1.345 ± 0.023	1.150 ± 0.019	1.161 ± 0.020
Lu	0.353 ± 0.008	0.324 ± 0.005	0.207 ± 0.004	0.274 ± 0.005	0.190 ± 0.004	0.162 ± 0.003	0.165 ± 0.003
Zr	71 ± 15	68 ± 15	27 ± 6	50 ± 11	(<18)	15 ± 5	19 ± 5
Hf	1.98 ± 0.05	1.82 ± 0.05	0.734 ± 0.022	1.60 ± 0.03	0.489 ± 0.015	0.444 ± 0.014	0.436 ± 0.015
Ta	0.416 ± 0.014	0.378 ± 0.013	0.135 ± 0.006	0.540 ± 0.015	0.106 ± 0.005	0.083 ± 0.004	0.088 ± 0.005
U	1.49 ± 0.09	1.58 ± 0.04	0.270 ± 0.018	2.56 ± 0.08	0.81 ± 0.03	0.499 ± 0.029	0.431 ± 0.021
Th	1.30 ± 0.03	0.861 ± 0.020	0.557 ± 0.015	1.95 ± 0.03	0.489 ± 0.012	0.419 ± 0.010	0.473 ± 0.013
As	5.7 ± 0.3	2.23 ± 0.09	0.56 ± 0.06	11.0 ± 0.3	1.02 ± 0.08	0.54 ± 0.06	0.88 ± 0.06
Se	2.11 ± 0.21	1.24 ± 0.18	0.89 ± 0.11	1.36 ± 0.19	0.39 ± 0.09	0.13 ± 0.07	0.68 ± 0.12
Sb	1.123 ± 0.025	0.624 ± 0.013	0.286 ± 0.008	0.700 ± 0.015	0.208 ± 0.007	0.201 ± 0.006	0.201 ± 0.006
Parts per billion							
Ir	(<0.8)	(<0.7)	(<0.4)	2.0 ± 0.4	(<0.4)	(<0.3)	(<0.4)
Au	6.7 ± 1.4	6.2 ± 0.7	0.80 ± 0.30	2.8 ± 0.7	1.23 ± 0.18	0.8 ± 0.3	11.3 ± 0.6